ISSN 1392-1207. MECHANIKA. Vol. 32, No. 3, 2026: 208–219

Design of the Complex Aluminum Bridge Extrusion Die Through Finite Element Analysis

Yunus SARAL*, Sait Özmen ERUSLU, Ibrahim Savaş DALMIS*****

**Tekirdağ Namık Kemal University, Çorlu Faculty of Engineering, Mechanical Engineering Department, 59860, Çorlu-Tekirdağ, Türkiye, E-mail: saralyunus61@gmail.com*

***Tekirdağ Namık Kemal University, Çorlu Faculty of Engineering, Mechanical Engineering Department, 59860, Çorlu-Tekirdağ, Türkiye, E-mail: oeruslu@nku.edu.tr*

****Tekirdağ Namık Kemal University, Çorlu Faculty of Engineering, Mechanical Engineering Department, 59860, Çorlu-Tekirdağ, Türkiye, E-mail: idalmis@nku.edu.tr (Corresponding Author)*

https://doi.org/10.5755/j02.mech.44593

1. Introduction

The aluminum extrusion process is a manufacturing method that aims to produce profiles by forcing a block-shaped raw material, called a billet, through a die under high pressure. Therefore, extruding an aluminum profile requires high-capacity presses while ensuring that the produced profile has the lowest acceptable level of defects. For this reason, the dies used in the extrusion process play a crucial role in both the process itself and the quality of the final product. These dies are made from hot-work tool steels that are resistant to high temperatures, have high strength, and exhibit excellent wear resistance. Die design is typically carried out through a trial-and-repair process based on the knowledge and experience of the die designer. Therefore, to reduce the time, waste, and costs associated with this trial-and-error process, numerical analysis applications have recently gained attention.

In the extrusion process, the goal is to produce products with uniform cross-sections. To achieve this, the melting flow is balanced by ensuring a more uniform velocity across the entire die with a pressure drop. Optimize the flow to prevent sudden changes in the passage that could result in stagnant areas. Stagnation can cause the plastic to degrade thermally due to prolonged exposure to high temperatures [1].

Hollow profile extrusion is an advanced forming process widely employed to manufacture lightweight components with complex cross-sectional geometries. Unlike solid extrusion, it requires porthole dies, where the billet is divided by mandrel support and subsequently rejoined under high pressure in a welding chamber. This rejoining process forms longitudinal weld seams, the quality of which strongly influences the mechanical performance of the extrudate. The die bearing length further governs the material flow, dimensional accuracy, and surface finish of the final profile. Due to its efficiency in producing structurally optimized shapes, hollow profile extrusion has found extensive applications in the transportation, construction, and aerospace industries. However, challenges such as uneven flow distribution, seam weld integrity, and high die stresses necessitate careful die design and process optimization.

The areas of the portholes in the extrusion die must correspond to those of the respective regions of the extrudate to ensure proper material distribution. In addition, the width of the drainage channel should be maximized to enhance material supply, while still maintaining sufficient die strength [2].

Porthole die design consists of a mandrel supported by multiple portholes (legs or bridges), through which the metal flows before rejoining in the welding chamber. As the aluminum billet passes around the bridges, it is divided into multiple streams and then undergoes solid-state welding under high pressure before being extruded into the final profile shape.

In the extrusion process, dies play an important role in material flow homogeneity, and the mold directly affects the quality of the profile. The material flow in molds is balanced through various methods given at literature. The design of the porthole die should ensure optimal material flow and a uniform temperature distribution to achieve the desired profile and minimize die scrap. Uniform material flow also plays a crucial role in the quality of weld lines in extruded parts [3].

Liu et al. investigated the design of the porthole die for extrusion profiles with high length-to-width ratios and small cavities. In their study, material flow was balanced with baffle plates, welding chambers were rearranged, and angles of portholes were increased [4].

Fang et al. focused on the porthole die design for the extrusion of thin-walled, flat, multi-port aluminum tubes. They optimized the mandrel structure, specifically addressing the effects of uneven deflection of the mandrel teeth, and improved the die bearing length, which is a key factor in non-uniform metal flow [5]. Llorca-Schenk et al. developed mathematical regression equations to optimize material flow in the design of cavities in porthole dies for aluminum extrusion processes, reducing computational effort in FEM analysis [6]. Nguyen and coworkers (2024) analyzed the complex porthole die design for the poorly extrudable 7000 series aluminum extrusion [7]. In their study, revisions were made to the bearing length, die runout, and pocket shape to enhance material flow and extrusion performance. Bridge die design features a single or multi-bridge mandrel that supports the core, forming a hollow shape. Metal flows around the bridges, rejoins before exiting the die, and undergoes welding in a less confined chamber compared to porthole dies, typically with fewer segments in the metal flow. This technique is suitable for larger hollow sections and high-strength applications. Ayer et al. conducted a study in which they performed the extrusion simulation of a hollow die for a box profile using the FEM-based HyperXtrude Inspire Extrude Metal program. They evaluated the die design based on the shape of the bridges and conducted the simulation accordingly. As a result, it was found that dies with inclined bridges provided optimal processing conditions [8]. Wang et al. studied the influence of bridge geometry on the complex hollow aluminum cross-section in Al alloy extrusions [9]. The study showed that bridge geometry had a significant effect on material flow, local microstructure, and crystallographic texture at the weld line. Another important factor in material flow optimization is the pocket in die design, which is generally used in the lower die plate, in front of the die opening, to regulate the flow of metal [10]. Donati et al. focused on pocket shapes in the multi-hole die aluminum extrusion process. The study compared the material flow rates of conical and stepped pocket shapes [11]. You Feng et al. examined the impact of pockets in the porthole die on metal flow and extrusion load in the aluminum extrusion process [12]. Hsu, Chen, and Lee investigated the extrusion process by modifying the pocket geometry and cavities to achieve uniform material flow, and, to establish an improved bridge-type extrusion die design, they employed the DEFORM-3D finite element analysis program in conjunction with the Taguchi method [13]. Güngördü examined the effects of die temperature and pocket pool dimensions on material flow and die life in the aluminum extrusion process using the finite element code QForm [14]. Increasing the welding pressure and improving the quality of welding products are very important issues in the hollow die extrusion of aluminum [15]. Elongating the welding chamber and bearing length is an important way to increase welding pressure [16]. Chen and coworkers studied the effects of increasing the step of welding chambers on metal flow and weld quality in the aluminum extrusion of complex hollow profiles [17]. The study found that more uniform material velocity and temperature distribution are achieved by stepped welding chambers. Junquan Yu and coworkers investigated modular porthole extrusion dies with different depths of welding chambers to obtain optimum weld quality at L weld seams in extruded profiles [18]. Chan Ma and colleagues studied the welding lines in aluminum porthole extrusion by using the K value to account for negative pressure in the welding zone [19]. The welding line characteristics were evaluated using this criterion in the study. Wang and Wells investigated the effects of bridge angle on the weld seam and product quality in the porthole extrusion of aluminum profiles using FEM analysis [20]. Their study indicated that lower bridge angles directly affect material flow at the weld seam. Ayar and Karakaya focused on the design of the die to ensure welding quality in the porthole die extrusion of aluminum. The study included tensile tests, hardness measurements, and microstructural analysis to evaluate welding quality [21]. Hwang and Hsu focused on welding pressure and weld seam quality in the hollow die extrusion of aluminum profiles. Their research used FEM analysis and the Taguchi method to investigate the effects of die geometry on weld pressure [22]. Liu and coworkers studied the effects of billet temperature and ram speed on the microstructure of the longitudinal weld zone in the porthole die extrusion of aluminum [23]. Baffle plates and cavities in the die control material flow and improve extrusion uniformity by directing the metal smoothly, minimizing turbulence, and ensuring a consistent flow. Zhang et al. investigated the aluminum extrusion process both numerically and experimentally using the HyperXtrude program. In their study, they achieved a precise dimensional profile by adjusting the arrangement, shape, and height of the baffle plates [24]. Jie and coworkers focused on extrusion defects in porthole dies during the extrusion of complex aluminum profiles. The uniformity of metal flow is analyzed using FEM simulation, considering baffle plates for uniform distribution and varying heights of the welding chamber [25].

Although numerous studies have investigated porthole die extrusion and the influence of individual design parameters such as pocket geometry, bearing length, or bridge configuration, limited research has focused on the integrated optimization of bridge die designs for complex hollow aluminum profiles. In particular, the combined influence of baffle plates, pocket geometry, and bearing length on metal flow uniformity, welding pressure, and final product properties has not been comprehensively addressed. Moreover, many previous studies rely solely on numerical simulations without extensive experimental validation under industrial extrusion conditions.

Therefore, the present study aims to perform a comprehensive optimization of a complex aluminum bridge die by simultaneously modifying baffle plates, pocket geometry, and bearing lengths using finite element analysis. The numerical predictions are validated through industrial extrusion experiments, dimensional measurements, and mechanical testing of the extruded profiles. The study provides insights into the interaction between die design parameters and material flow behavior, and demonstrates a practical methodology for improving flow balance, weld quality, and dimensional accuracy in the extrusion of complex hollow aluminum profiles.

2. Porthole Die Design

Aluminum extrusion dies are generally used for solid profiles such as L-profiles, I-profiles, and flat bars, while bridge dies are used to manufacture hollow profiles. In the extrusion process, dies play a crucial role in ensuring the homogeneity of material flow. Any issue in the material flow within the die can directly affect the quality of the profile. Material flow in extrusion dies is balanced using various methods. For example, in bridge dies, the arrangement and shape of the chambers can be modified, fusion zones can be designed, different pocket lengths can be applied, or transition lengths within the die can be adjusted to regulate material flow. The bridge dies used in this study are shown in the following Fig. 1.

The chamber ensures that the raw material is distributed within the die in a specific manner to the desired locations. The number and position of the chambers may vary depending on the profile design. The bridge is a fundamental component that provides support between the chambers. The weld chamber is a section of the die where the raw material (aluminum) converges after passing through separate chambers. In the weld chamber, these streams are reunited and fused to form a single, continuous profile. The pocket chamber plays a role in stabilizing the flow, making final adjustments to the material distribution before it exits the die. This region is typically an additional cavity designed within the weld pool to regulate local flow differences in the profile and ensure controlled flow. The baffle plate is a physical feature inside the weld chamber. The main purpose of the baffle plate is to balance the stress in the material flow. This means that it helps to manage the pressure and force applied to the material as it moves through the chamber, ensuring it flows smoothly.

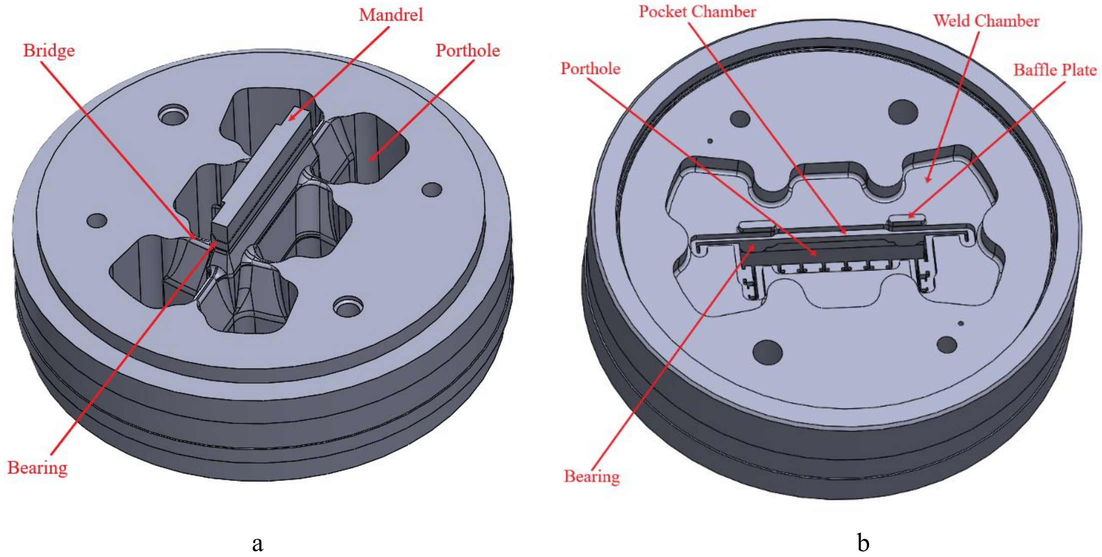

Fig. 1 Aluminum bridge die: a – upper die, b – lower die

3. Finite Element Modeling of Aluminum Die Extrusion

HyperXtrude Inspire Extrude Metal 2019 FEM code is used for finite element modeling of the aluminum extrusion process. A coupled-field thermomechanical simulation procedure is applied in the analysis, combining transient thermal effects with mechanical effects. Both steady-state and transient simulations were carried out to capture material flow and stabilization during cooling [7]. The Arbitrary Lagrangian-Eulerian (ALE) formulation is applied to the model, combining the advantages of both the Eulerian and Updated Lagrangian methods. The Eulerian (steady-state) approach uses a fixed mesh, which limits its ability to simulate the die-filling process, but it offers benefits such as reduced computational time. On the other hand, the Updated Lagrangian method allows for intuitive simulation of material flow, similar to what is observed in an extrusion press. By incorporating ALE, the model can effectively handle both accurate material flow representation and computational efficiency [26].

The aluminum extrusion simulation model is shown in the following Fig. 2.

An optimum mesh consisting of approximately 1.6 million tetrahedral elements was used in the finite element model to achieve a balance between computational efficiency and accurate representation of material flow during the extrusion process, as shown in Fig. 3.

In the aluminum extrusion process, H13 steel, known for its excellent wear resistance and high-temperature endurance, is used as the die material, while the billet material is AA 6061 aluminum alloy. The thermomechanical properties of H13 and AA 6061 materials are provided in Table 1 [27].

Table 1

The thermomechanical properties of H13 steel and AA 6061

Thermomechanical Properties	H13	AA6061
Young's modulus E, MPa	210	40
Poisson's ratio ν	0.35	0.35
Density, kg/m^3	7870	2700
Thermal conductivity, W/(m·k)	24.3	198
Specific heat, J/kg·K	460	900

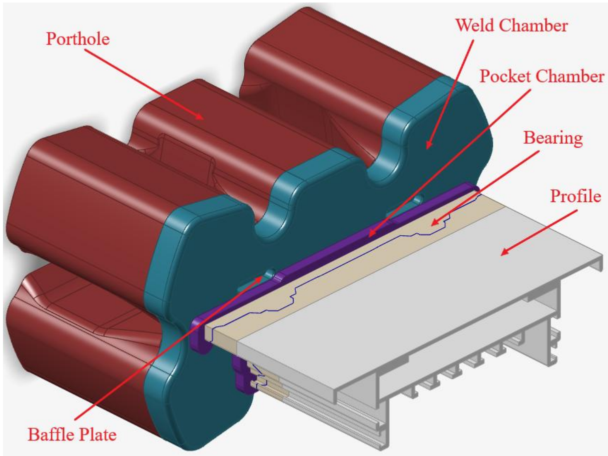

Fig. 2 Simulation model of aluminum bridge die extrusion

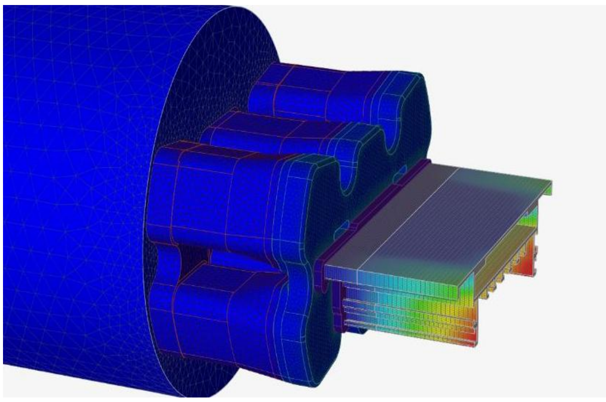

Fig. 3 Finite element model of aluminum porthole die extrusion

During the extrusion process, the aluminum billet is forced into the die cavity by the extrusion press under high temperature, high pressure, and high friction. Therefore, the metal flow within the die cavity is quite complex. To describe the high-temperature deformation behavior of aluminum alloys, the constitutive Sellars-Tegart model given in Eq. (1) is used [24]

$$\sigma = \frac{1}{\beta} sinh^{-1}\left[\left(\frac{\dot{\varepsilon} \times e^{Q/RT}}{A}\right)^{\frac{1}{n}}\right]. \quad (1)$$

In this model, σ denotes the flow stress of the material, while β is the reciprocal stress factor and A is the reciprocal strain rate factor. The term $\dot{\varepsilon}$ represents the effective strain rate, and n is the stress exponent. Additionally, the model incorporates the activation energy for deformation (Q), the universal gas constant (R), and the absolute temperature (T), The material parameters used in our study, based on the constitutive Sellars–Tegart model, are: $A = 5.91\times10^9$ s^{-1}, $Q = 1.416\times10^5$ J/mol, $R = 8.314$, $n = 5.385$ and $\beta = 4\times10^{-8}$ m^2/N [25]. The extrusion parameters used in the finite element analysis (FEA) are given in the Table 2.

Table 2

Table 2 Extrusion Parameters used in FEA

Billet diameter, mm	203
Billet length, mm	600
Billet temperature, °C	450
Die temperature, °C	450
Container temperature, °C	430
Extrusion ratio	35.06
Ram speed, mm/s	4
Friction coefficient between billet and die	0.3

Here, the billet diameter and length, as well as the billet, die, and barrel temperatures, along with the punch speed, are taken from the extrusion process. The extrusion ratio presented in the table is defined as the ratio of the billet cross-sectional area to the final profile cross-sectional area.

4. The FEA Results at First Die Design

The first die, which was designed and manufactured, was analyzed using finite element analysis, and the resulting material flow, profile exit speed, and exit temperature in the extrusion direction are shown in Fig. 4. In Aluminum 6063 alloys, the die exit temperature is desired to be between 500 and 550 °C. This is because exceeding this range may deteriorate the mechanical properties and microstructure of the material. In addition, excessive temperature can adversely affect the intended precipitate distribution during the aging process. According to the simulation results of the first manufactured die, high temperature values were obtained, with the maximum temperature in the flow occurring at the partition plates, reaching 573 °C.

In the extrusion process, the uniformity of the flow velocity at the die exit largely affects the quality of the extrusion profile. To quantify the degree of uniformity of the profile's exit velocity, the VRD (Velocity Relative Difference) is defined by the following Eq. (2) [10, 28]

$$VRD(\%) = \frac{\sum_{i=1}^{n} \frac{|v_i - v_a|}{v_a}}{n} \times 100 . \quad (2)$$

As a result of the calculations, the VRD value for the first designed die was approximately 25.3%. Due to the high VRD value, dimensional and geometric distortions were observed, particularly bending deformations and deviations in section dimensions. The first designed profile at the die exit is shown in Fig. 5.

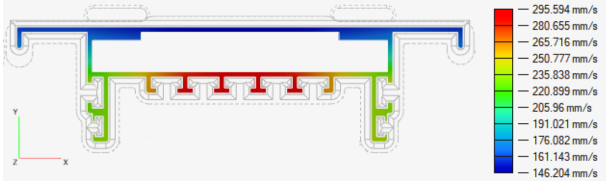

a

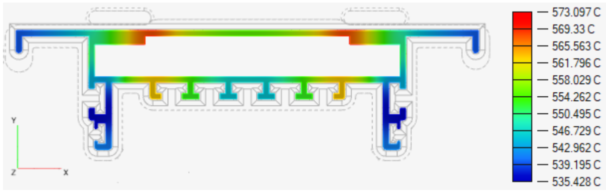

b

Fig. 4 Simulation results of the metal flow at the exit of the first designed die: a – velocity, b – temperature

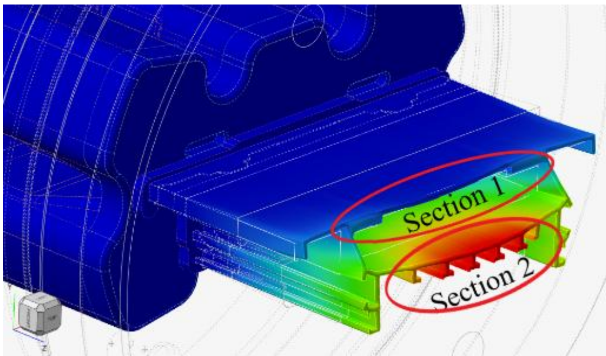

a

b

Fig. 5 The first designed profile at the die exit: a – FE analysis, b – extrusion process

5. Optimization Study of Extrusion Die

The optimization procedure was carried out through sequential design revisions based on FEM results. This approach reflects the practical industrial die design methodology, where die geometry is gradually improved according to simulation outcomes rather than using purely mathematical optimization techniques. Therefore, several die revisions were developed to systematically evaluate the effects of baffle plates, pocket geometry, and bearing length on material flow behavior. The initial and final designs used in the optimization studies conducted in this research are presented.

5.1. Baffle plates effects

In the initial design, baffle plates were incorporated within the welding chamber surrounding the extruded profile, in the regions corresponding to a wall thickness of 2 mm, to regulate material flow relative to the sections with a wall thickness of 5 mm. However, it was subsequently determined that the presence of these baffle plates impeded the material flow, leading to elevated temperatures because of frictional effects and increased pressure.

To systematically examine the influence of baffle plates on the extrusion process, two alternative die configurations were developed for the welding chamber of the lower die and evaluated within a simulation environment. These designs, designated as Design 1 and Design 2, are presented in Table 3 along with their corresponding illustrations and descriptions. Design 1 does not incorporate any baffle plates within the welding chamber, whereas Design 2 includes an additional baffle plate with dimensions of 5×35×5 mm positioned at the lower region adjacent to the die cavity, supplementary to the configuration of Design 1. The optimization studies conducted to investigate the effect of baffle plates are summarized in Table 3.

Table 3

Optimization studies to investigate the effect of baffle plates on the initial design

Die	Lower die	Explanation of the performed procedure
Design 1	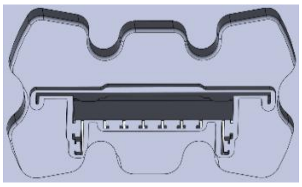	Removal of the baffle plates in Section 1 of the welding chamber
Design 2	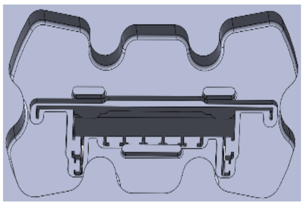	In addition to the baffle plates in Section 1, add a 35 mm long baffle plate to Section 2

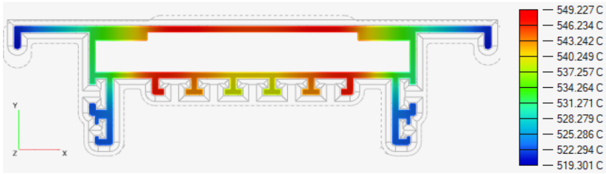

a

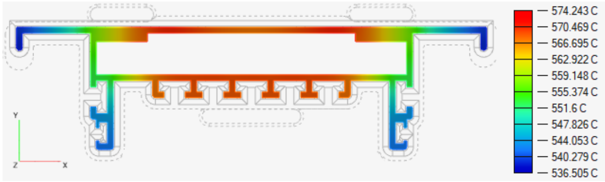

b

Fig. 6 Temperature distributions at the die exits: a – Design 1, b – Design 2

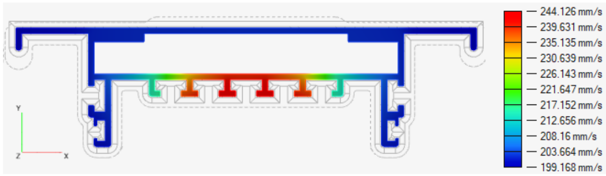

a

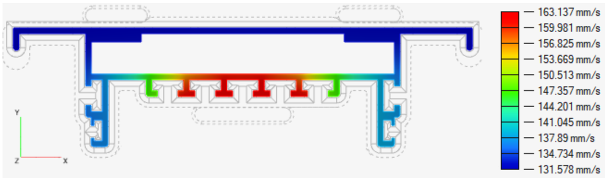

b

Fig. 7 Velocity distribution at the die exits: a – Design 1, b – Design 2

The simulation results for Design 1 and Design 2, illustrating the temperature distribution at the die exit, are presented in Fig. 6. The maximum exit temperature recorded for Design 1 was 549 °C, while that of Design 2 was 574. Given the absence of baffle plates in the welding chamber of Design 1, lower exit temperatures were attained in comparison to the initial design, and these temperatures were deemed adequate for the successful extrusion of the profile. In contrast, the baffle plates present in Design 2 contributed to elevated exit temperatures, attributable to the frictional resistance and pressure buildup during material flow. Notably, the baffle plate introduced in Section 2 was observed to locally increase the temperature in that region by approximately 15-20 °C.

The velocity distributions at the die exit for Design 1 and Design 2, derived from the simulation results, are illustrated in Fig. 7. The velocity ratio deviation (VRD) was determined to be 9.3% for Design 1 and approximately 9.6% for Design 2, both of which remain within the industrially accepted threshold of 10%. Although the incorporation of baffle plates reduced the profile exit velocity, the plates positioned at the upper and lower regions of the welding chamber contributed to a more balanced flow distribution, yielding a VRD value comparable to that of the baffle-plate-free configuration.

The welding pressure distributions within the welding chambers of the investigated dies are presented in Fig. 8. As is evident from the results, the pressure in the welding regions is comparatively lower than in the surrounding areas. Upon examination of the welding pressures within the welding chamber, the average welding pressure in the initial design was determined to be 215.5 MPa, whereas that of the final die configuration reached 228.3 MPa. The average welding pressure obtained in Design 2 is approximately 6% higher than that recorded in Design 1, with a further localized increase in welding pressure observed in the vicinity of the baffle plates. This phenomenon is attributed to the elevated metallic flow resistance experienced by the material as it advances toward the die cavity. The incorporation of baffle plates promotes a more uniform flow distribution, thereby enhancing the metallurgical bonding conditions and improving overall weldability.

In addition to the welding pressure analysis, the mechanical properties of the extruded profiles were assessed through uniaxial tensile testing and hardness measurements.

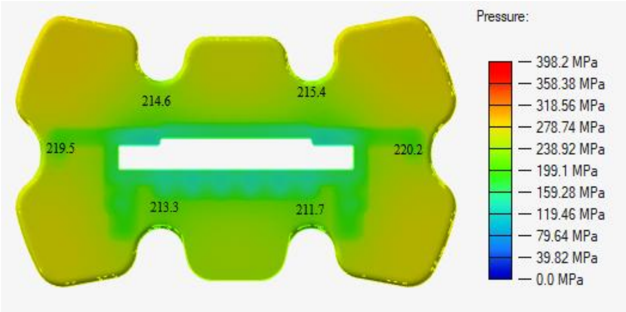

a

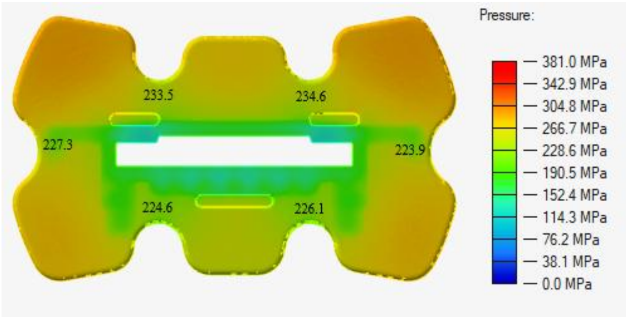

b

Fig. 8 Welding pressure in the welding chambers of the die: a –Design 1, b – Design 2

The absence of fracture initiation along the weld seams during tensile testing confirms that the welding quality achieved throughout the extrusion process was metallurgically sufficient and meets the required structural integrity criteria.

In Design 1, non-uniform material flow distribution resulted in extrusion defects, including profile bending and dimensional deviations in the cross-section, accompanied by elevated exit temperatures. The baffle plate incorporated at Section 1 in the initial design impeded the material flow, consequently inducing localized temperature increases attributable to frictional effects. The introduction of an additional baffle plate at Section 2 in Design 2 yielded a more balanced flow distribution; however, the results remained inconsistent with the target specifications. A similar outcome was observed in the configuration where the baffle plates were entirely eliminated from Design 1, which likewise failed to produce the desired flow characteristics.

These results indicate that evaluating the baffle plate alone is not sufficient for die optimization. A more reliable improvement in flow distribution can be achieved by considering it together with other die design parameters. In extrusion die design, parameters such as bearing length, pocket geometry, and baffle plates interact with each other and collectively influence the metal flow distribution.

5.2. Integrated effect of considering bearing length, pocket design, and baffle plates

In this section, a comprehensive optimization considering bearing length, pocket design, and baffle plates was carried out, and the final revision of the die was developed. The die previously defined as Design 1 in the earlier section is referred to as the initial design in the subsequent sections.

5.2.1. Revision of bearing lengths

Bearing lengths are the final regions where the profile is formed and thus play an important role in the design process of the extrusion die. Proper arrangement of the bearing lengths directly affects the quality of the final extruded product. Since these lengths represent the last region before the material enters the die cavity, minimizing friction in problematic areas has been established as a primary objective. The aim is to reduce the temperature in the region and to balance the material flow by minimizing friction. The bearing lengths within the red square shown in Fig. 9 were modified to form the final bearing lengths.

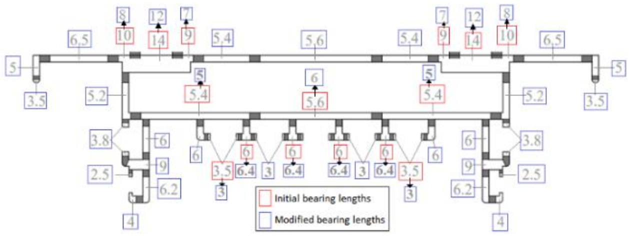

Fig. 9 Revision of bearing lengths

5.2.2. Modification of the pocket design

The pocket is a region where the material flows after the welding chamber to improve profile quality. This area is designed as an additional cavity within the welding chamber, primarily to regulate local flow variations in the profile and to ensure controlled material flow. In the initial die, the pocket was designed 4 mm away from the outer positions of the extruded profile, while the section with baffle plates was adapted 2 mm away from the profile.

Fig. 10 presents a comparison between the initially designed and the modified pocket. The purpose of the redesigned pocket is to enhance the material flow into Section 1 and resolve the slow flow issue. For this reason, the upper baffle plates were removed, and the pocket was widened by 2 mm.

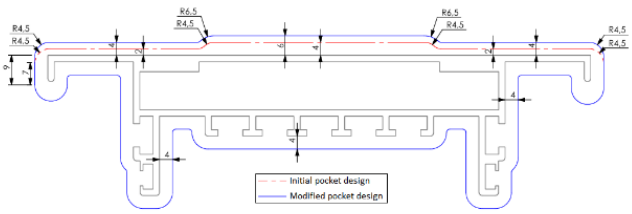

Fig. 10 Comparison of initial and modified pocket design

5.2.3. Baffle plate optimization

In the initial design, baffle plates were added to distribute the flow more uniformly toward the sections of the extruded profile with a wall thickness of 5 mm; however, the intended results were not achieved. To evaluate the effect of the baffle plates, analyses of the initial design and final design dies were performed, and the results indicated that the plates slowed the flow and increased the temperature due to frictional effects. Consequently, since the flow in Section 1 of the initial design was significantly slower, the baffle plates in this region were removed, the pocket depth was increased by 2 mm, and the bearing lengths were shortened by 2 mm. In order to balance the relatively higher

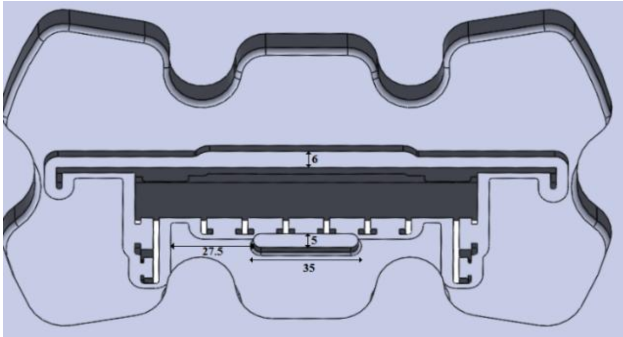

Fig. 11 Lower die after revision design

material flow in Section 2, as shown in Fig. 11, an additional baffle plate with dimensions of 5 × 35 × 5 mm was incorporated, considering a symmetric and uniform thickness design.

5.2.4. Simulation results of the last revised die

The simulation of the revised die was performed using FEA, and the resulting profile exit temperature and exit velocity are presented in Fig. 12. The welding pressure of the revised die is shown in Fig. 13.

The average pressure in the welding regions is 226.7 MPa, which is approximately five times higher than the effective stress of the welded material (45 MPa), indicating that the weld quality of the extruded profile is satisfactory.

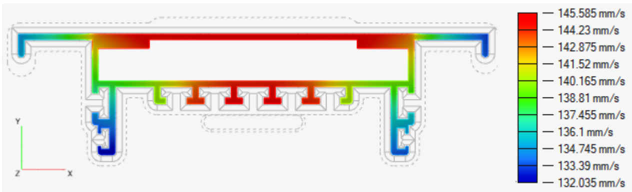

a

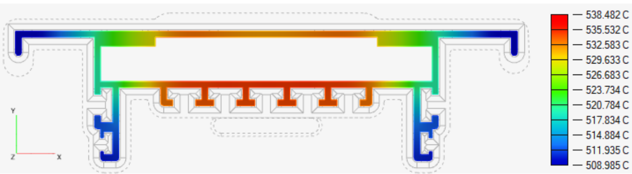

b

Fig. 12 Simulation results of the metal flow at the exit of the revised die: a – temperature, b – velocity

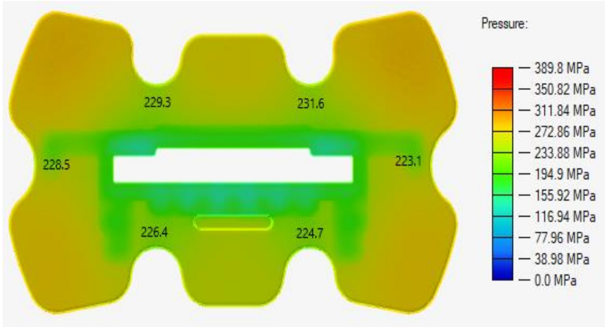

Fig. 13 Welding pressure in the welding chamber of the revised die

When examining the effect of the modifications on the results, the reduction of the high temperature and high flow rate at the upper part of the extruded profile was achieved by widening the pocket chamber by 2 mm, shortening the bearing lengths in the upper region, and removing the baffle plates. Through all three revisions, friction and pressure were reduced, temperature values decreased, and the flow rate increased at Section 1. In addition, a baffle plate was added to section 2 of the extruded profile, which reduced the high velocity and helped to balance the material flow.

5.3. Comparison of the revised die with the initially designed die

The velocity distribution at the die entry of the initially designed and revised dies is shown in Fig. 14. Examination of the color scale indicates that the metal flow velocity in the revised die has become more uniform. The reduction in velocity in Section 2 can be attributed to the widening of the pocket, the modification of bearing lengths in Section 1, and the addition of a baffle plate in Section 2. These adjustments altered the material flow orientation and reduced local flow variations. As a result of the modifications made in the revised die, the VRD value decreased from 25.3% in the initial die design to 4.6%.

The velocity curves at the designated reference points in Fig. 14 are presented in Fig. 15 for both the initial and revised designs. It was observed that the velocity difference was significantly reduced in the revised die design compared to the initial one, and that modifications to the baffle plates, pocket, and bearing lengths enabled effective control of the metal flow.

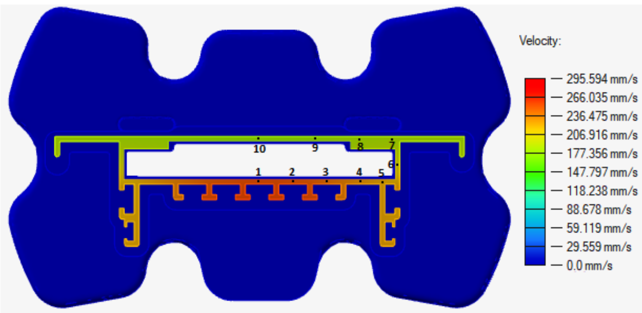

a

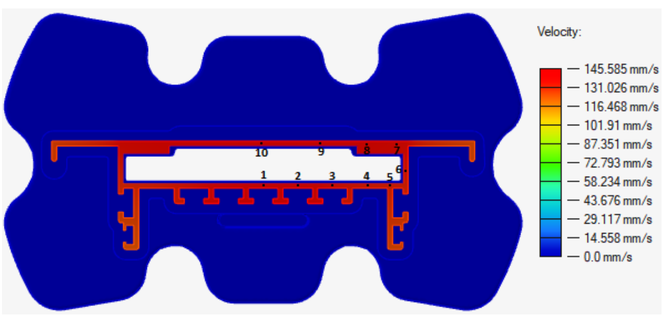

b

Fig. 14 Comparison of the material velocity at the inlet of the die orifice: a – initial die, b – revised die

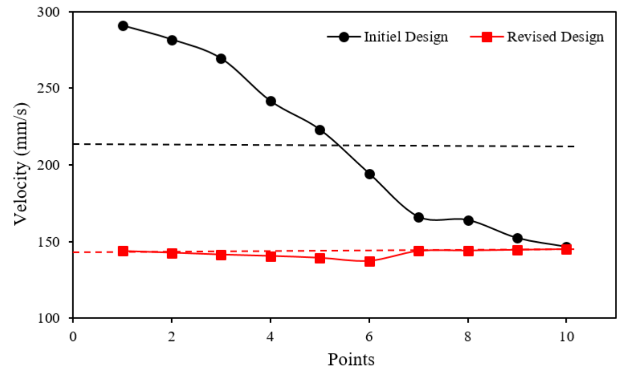

Fig. 15 Velocity curves of the reference points

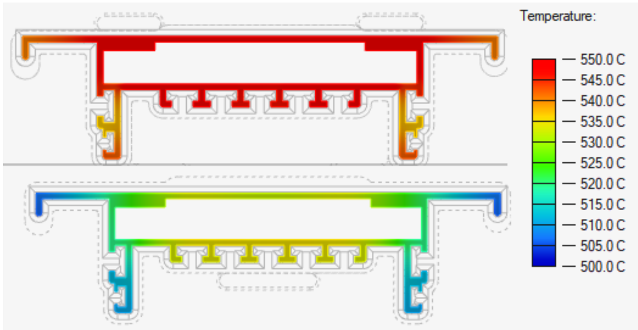

Fig. 16 Temperature distributions in die of initial and revised design

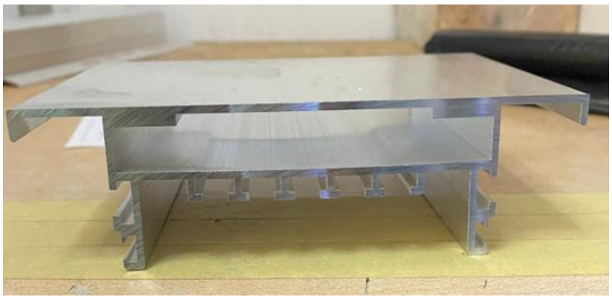

Fig. 17 The extruded profile after die revisions

A comparison between the initial and revised designs in terms of exit temperature within the 500-570 °C color scale is presented in Fig. 16. In the initial design, a large portion of the exit area exceeded 550 °C, while in the revised die obtained through optimization studies, the temperature was maintained within the desired range. This indicates that modifications to the baffle plates, pocket, and bearing lengths also affected the temperature distribution.

After producing the defective product with the initial design, a successful extrusion process was achieved using the revised die obtained through optimization studies, resulting in the final product shown in Fig. 17.

The dimensions of the profiles produced from both the revised and the initial die designs were measured with high precision using a two-dimensional measurement projection system, the Romidot device, which enables automatic inspection of profile geometry.

The reference dimensions of the extruded profile are shown in Fig. 18. The dimensions of the profiles produced from the revised die and the initial die were measured with high precision using the two-dimensional measurement projection system Romidot, which enables automatic inspection of profile geometry. Some sections of the profile

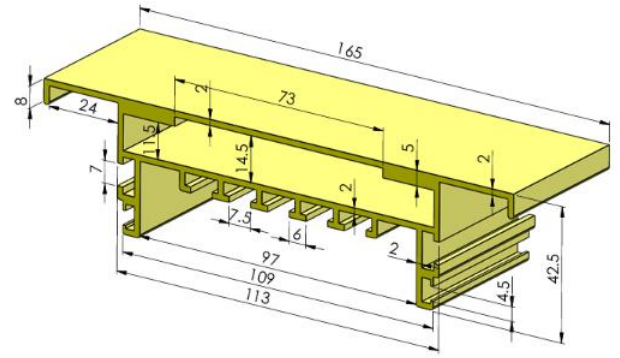

Fig. 18 The reference dimensions of the extruded profile

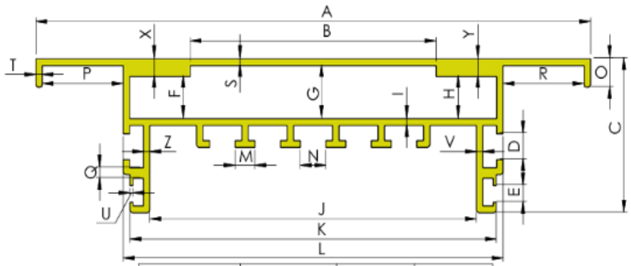

Dimension	Desired Tolerance	Initial Design	Revised Design
A	± 1,00	164,461	164,836
B	± 0,45	72,542	73,064
C	± 0,30	42,483	42,466
D	± 0,15	6,906	6,907
E	± 0,15	4,491	4,492
F	± 0,20	11,662	11,654
G	± 0,20	14,593	14,627
H	± 0,20	11,621	11,618
I	± 0,40	1,854	1,85
J	± 0,60	97,615	97,416
K	± 0,60	109,647	109,472
L	± 0,60	113,244	112,906
M	± 0,15	6,014	5,982
N	± 0,15	7,618	7,526
O	± 0,15	7,984	7,985
P	± 0,25	24,269	24,076
Q	± 0,15	2,957	2,954
R	± 0,25	24,289	23,995
S	± 0,40	1,927	1,93
T	± 0,25	1,919	1,947
U	± 0,15	0,94	0,94
V	± 0,25	1,831	1,837
X	± 0,60	4,812	4,858
Y	± 0,60	4,806	4,826
Z	± 0,25	1,895	1,872

Unit: mm

Fig. 19 Measured dimensions of the extruded profile

produced using the initial die design were found to be outside the specified tolerance limits. The reference dimensions of the profile were obtained from the manufacturer, as illustrated in Fig. 19.

In particular, the B, J, K, P, and R dimensions, which were out of tolerance in the initial design die, were found to fall within the desired tolerances of the final product after the revision. The out-of-tolerance dimensions observed in the initial design die are attributed to the extrusion speed in the corresponding sections.

Another important aspect of the extrusion process is the effect of die optimization on the extrusion force. In bridge dies, knowing the extrusion force is crucial for determining the capacity of the press to be used and for ensuring a successful extrusion operation. Therefore, the extrusion forces of the initial die and the revised die were calculated both in the simulation environment and experimentally, and the results are presented in Table 4. During the extrusion experiments, the formula given in Eq. (3) was used to calculate the extrusion force, and the pressure values of the main and auxiliary cylinders were taken into account to convert the data into force units

$$F = \left(\frac{\pi \times D^2}{4} + 2 \times \frac{\pi \times d^2}{4} \right) \times P \,. \quad (3)$$

Here, D is denotes the diameter of the main cylinder of the hydraulic press (1120 mm), d is represents the diameter of the auxiliary cylinder (250 mm), and P is indicates the total pressure measured in the cylinders. The calculated forces obtained from the experiments and simulations are presented in Table 4.

Table 4
Experimental and numerical extrusion force results of the initial and revised dies.

Die	Initial die	Revised die
Maximum cylinder pressure, kg/cm^2	172	161
Experimental force, tons	1863	1744
Simulation force, tons	1701	1679
Difference, %	9.5	3.8

An initial examination of the simulation results indicates that the obtained extrusion forces of 1679 and 1701 tons are below the maximum capacity of the 2600-ton extrusion press, suggesting that a successful extrusion process can be performed with this press.

5.4. Strength and displacement of revised die

In the extrusion process, extrusion dies are exposed to high temperatures, high pressures, and high-friction conditions, which can lead to deformation and cracking. For this reason, strength checks are necessary to ensure a longer service life and to mitigate these risks. Fig. 20 shows the stress distribution in the revised die. Although the upper die experienced higher stress than the lower die, the highest stresses occurred particularly at the porthole bridges. The maximum stress reaches 751 MPa at the porthole bridges, which is lower than the yield strength of H13 steel (834 MPa at 600 °C).

Fig. 21 shows the displacement of the revised die. The maximum displacement was observed at the tip of the mandrel in the upper die. The maximum displacement in the upper die is 0.141 mm, while in the lower die it is 0.057 mm. Since these deviations in the upper and lower dies of the revised design are within a safe range and no plastic deformation occurs, the revised die can be used for practical production.

5.5. Strength of extruded profiles

Tensile test specimens were prepared, as illustrated in Fig. 22, after the T66 aging heat treatment was applied to the profiles extruded from both the revised and the initial die designs. According to the tensile test results, the profile extruded from the initial die design exhibited a tensile strength of 226.6 MPa, a yield strength of 202.5 MPa, and an elongation of 9.4%, whereas the profile extruded from the revised die design showed a tensile strength of 246.9 MPa, a yield strength of 214.1 MPa, and an elongation of 11.2%. These results indicate that the revised die design not only enhanced the tensile and yield strengths but also improved the ductility of the extruded profiles. The simultaneous increase in strength and elongation demonstrates that the modifications made to the die contributed to a more favorable balance between strength and formability.

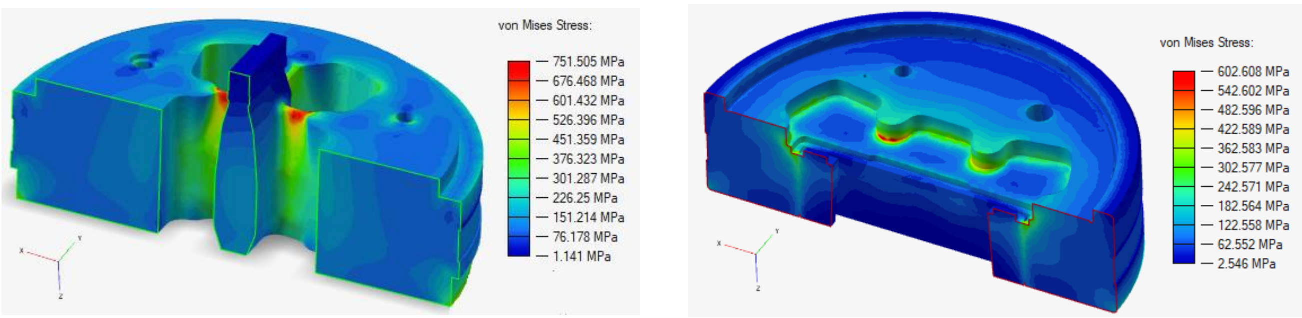

a b

Fig. 20 Stress distribution on the revised die: a – upper die, b – lower die

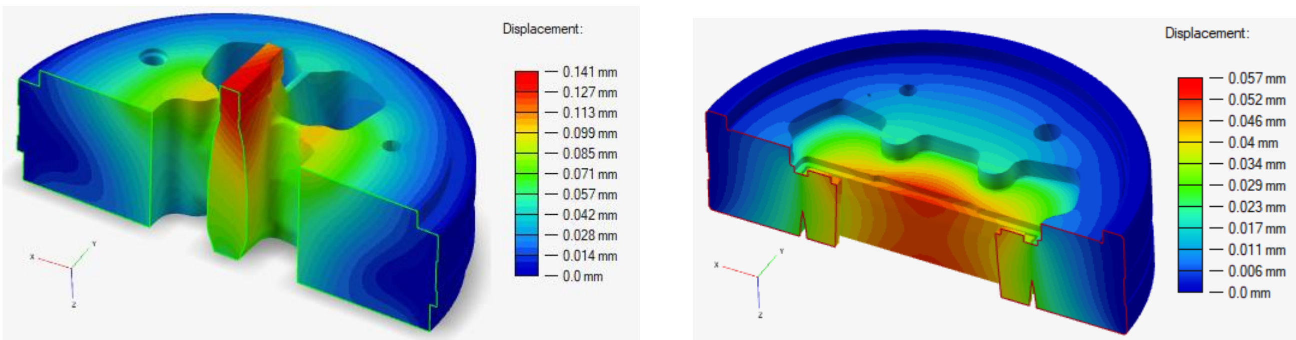

a b

Fig. 21 Die displacement of revised die: a – upper die, b – lower die

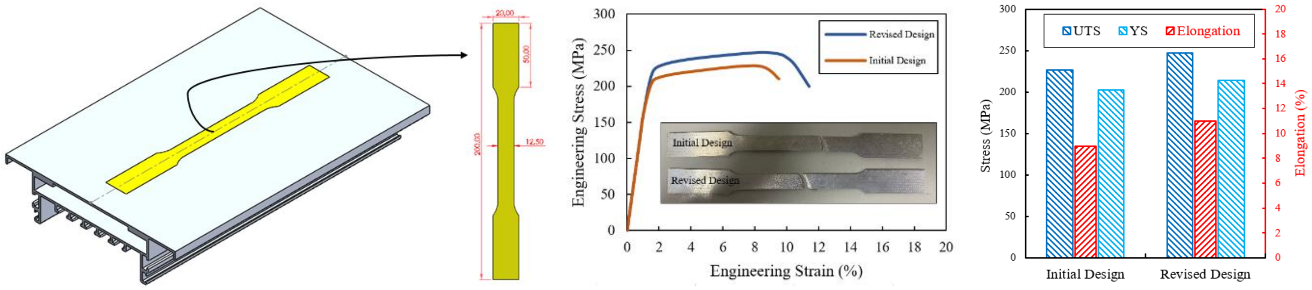

a b c

Fig. 22 Tensile test results: a – specimen dimensions, b – stress-strain curves, c – mechanical properties

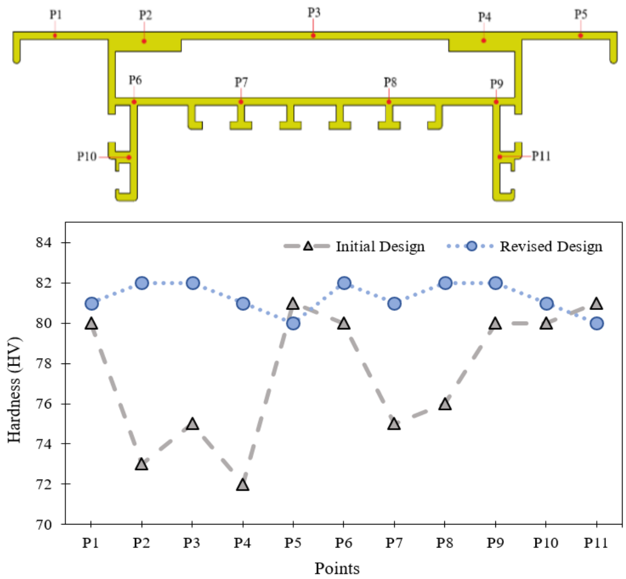

Fig. 23 Hardness measurement results at selected points

After applying the T66 aging heat treatment, hard measurements were carried out at specific points, as shown in Fig. 23 on the profiles extruded from both the revised and the initial die designs. According to the results, hardness values between a minimum of 80 HV and a maximum of 82 HV were measured at the designated points in the revised die, whereas the values ranged from a minimum of 72 HV to a maximum of 81 HV in the initial die. Typical Hardness Values for 6061-T66; however, in the product extruded from the initial die, the hardness values at points P2, P3, P4, P7, and P8 decreased by approximately 10%. Analysis of the simulation results indicated that, in the initial die, the exit temperatures at these locations exceeded 560 °C. Such elevated temperatures negatively influenced the aging process and prolonged the cooling period, ultimately resulting in a reduction of hardness at these points.

6. Conclusions

A comprehensive investigation was carried out to optimize the bridge die extrusion process for A6061 aluminum alloys using finite element analysis (FEA) combined with experimental validation. The initial die design exhibited significant flow imbalance, with high exit temperatures reaching approximately 573 °C and a velocity relative difference (VRD) of about 25.3%. These conditions resulted in extrusion defects such as profile bending, dimensional deviations, and out-of-tolerance sections. In addition, the welding pressure generated in the initial configuration was insufficient to ensure reliable weld seam formation.

The optimization study focused on the combined influence of baffle plates, bearing lengths, and pocket geometry on the metal flow behavior. The intermediate initial design and final design revisions showed that removing or repositioning the baffle plates and modifying the welding chamber configuration partially improved the flow balance and welding pressure distribution. However, localized flow variations and temperature increase remained.

In the final optimized die design, several modifications were implemented simultaneously, including shortening the upper bearing lengths, widening the pockets, and introducing baffle plates in high-flow regions. These combined changes significantly improved the flow balance, reducing the VRD from 25.3% to 4.6%. In addition, the exit temperature was maintained within the desired range of 500-550 °C, while the average welding pressure increased to approximately 226.7 MPa, which is well above the effective stress required for sound solid-state welding.

Mechanical characterization of the extruded profiles confirmed the effectiveness of the optimized die design. The tensile strength increased from 226.6 MPa to 246.9 MPa, the yield strength from 202.5 MPa to 214.1 MPa, and the elongation from 9.4% to 11.2%. Hardness measurements also showed more uniform values (80-82 HV) across the profile compared with the initial die, indicating a more consistent microstructural response during the extrusion process.

The structural integrity of the die was also verified through FEA. The maximum die stress was approximately 751 MPa at the porthole bridges, while the maximum displacements were 0.141 mm in the upper die and 0.057 mm in the lower die. These values remain within safe limits, indicating that the optimized design is suitable for practical industrial application and long service life.

Overall, the results demonstrate that the optimization of extrusion dies should not rely on individual design parameters alone. Instead, a coordinated modification of bearing lengths, pocket geometry, and baffle plates is required to achieve balanced metal flow, adequate welding pressure, and uniform temperature distribution. The combined use of numerical simulation and experimental validation provides a reliable methodology for improving both the performance and durability of complex aluminum extrusion dies while ensuring high-quality extruded profiles.

Acknowledgements

Support provided by Kurtoğlu Copper and Lead Industry Inc. during the experimental phases of this study is gratefully acknowledged. In addition, the student version of the Inspire Extrude Metal software developed by Altair was used in the simulation phases of this study, and sincere thanks are extended for granting permission for its use in this academic work.

References

1. **Kostic, M.M.; Reifschneider, L.G.** 2006. Design of Extrusion Dies, Encyclopedia of Chemical Processing 10: 633-649.
2. **Chen, H.; Zhao, G.; Zhang, C.; Guan, Y.; Liu, H.; Kou, F.** 2011. Numerical Simulation of Extrusion Process and Die Structure Optimization for a Complex Aluminum Multicavity Wallboard of High-Speed Train, Materials and Manufacturing Processes 26: 1530-1538. https://doi.org/10.1080/10426914.2011.551950.
3. **Lv, J.; Shi, Z.; Yu, J.; Li, W.; Lin, J.** 2023. Analysis of solid-state welding in extruding wide aluminium hollow profiles using a new three-container extrusion system, Journal of Manufacturing Processes 94, 146-158. https://doi.org/10.1016/j.jmapro.2023.03.048.
4. **Liu, Z.; Li, L.; Li, S.; Yi, J.; Wang, G.** 2018. Simulation Analysis of Porthole Die Extrusion Process and Die Structure Modifications for an Aluminum Profile with High Length–Width Ratio and Small Cavity, Materials 11(9): 1517. https://doi.org/10.3390/ma11091517.
5. **Fang, W.; Tang, D.; Wang, H.; Li, D.; Peng, Y.** 2020. Optimization of die design for thin-walled flat multi-port tube with the aid of finite element simulation, Journal of Materials Processing Technology 277: 116418. https://doi.org/10.1016/j.jmatprotec.2019.116418.
6. **Llorca-Schenk, J.; Sentana-Gadea, I.; Sánchez-Lozano, M.** 2021. Design of porthole aluminum extrusion dies through mathematical formulation. Materials Today Communications 27: 102301. https://doi.org/10.1016/j.mtcomm.2021.102301.
7. **Nguyen, T.-C.; Truong, T.T.; Wang, J.-W.; Sheu, J.-J.; Hsu, C.-L.; Hsu Q.-C.** 2024. Analyzing and enhancing the porthole die design for extruding a complicated AA7005 profile, The International Journal of Advanced Manufacturing Technology 134: 4803-4820. https://doi.org/10.1007/s00170-024-14439-1.
8. **Ayer O.; Ozmen B.G.; Karakaya I.** 2019. An Optimization Study for Bridge Design of a Porthole Extrusion Die, Advances in Science and Technology Research Journal 13(4): 270-275. https://doi.org/10.12913/22998624/115109.
9. **Wang, Y.; Zang, A.; Mahmoodkhani, Y.; Wells, M.; Poole, W.; Parson, N.** 2021. The Effect of Bridge Geometry on Microstructure and Texture Evolution During Porthole Die Extrusion of an Al–Mg–Si–Mn–Cr Alloy. Metallurgical and Materials Transactions A 52: 3503-3516. https://doi.org/10.1007/s11661-021-06322-5.
10. **Truong, T.-T.; Hsu, Q.-C.; Tong, V.-C.; Sheu, J.-J.** 2020. A Design Approach of Porthole Die for Flow Balance in Extrusion of Complex Solid Aluminum Heatsink Profile with Large Variable Wall Thickness, Metals 10(5): 553. https://doi.org/10.3390/met10050553.
11. **Donati, L.; Tomesani, L.; Shikorra, M.** 2009. The effect of pocket shape in extrusion dies, International Journal of Material Forming 2: 97. https://doi.org/10.1007/s12289-009-0454-4.
12. **He, Y.F.; Xie, S.S.; Cheng, L.; Huang, G.J.; Fu, Y.** 2010. FEM simulation of aluminum extrusion process in porthole die with pockets, Transactions of Nonferrous Metals Society of China 20(6): 1067-1071. https://doi.org/10.1016/S1003-6326(09)60259-4.
13. **Hsu, Q.C.; Chen, Y.L.; Lee, T.H.** 2014. Non-symmetric Hollow Extrusion of High Strength 7075 Aluminum Alloy, Procedia Engineering 81: 622-627. https://doi.org/10.1016/j.proeng.2014.10.050.
14. **Gungordu, F.** 2019. Alüminyum Ekstrüzyon Kalıp Tasarımı ve Sonlu Elemanlar Yöntemi ile Analizi (Aluminum extrusion die design and simulation by finite element method). Master of Science Thesis, Department of Mechanical Engineering, Gebze Technical University, Graduate School of Natural and Applied Sciences, Türkiye.
15. **Hsu, Q.C.; Tsai, P.H.** 2010. Study on the Guiding Chamber Effect on Welding Pressure in Hollow Extrusion Die Design, Proceedings of IMECE10, 2010 ASME International Mechanical Engineering Congress and Exposition 3: 619-624. https://doi.org/10.1115/IMECE2010-40030.
16. **Kim, K.J.; Lee, C.H.; Yang, D.Y.** 2002. Investigation into the improvement of welding strength in three-dimensional extrusion of tubes using porthole dies, Journal of Materials Processing Technology 130-131: 426-431. https://doi.org/10.1016/S0924-0136(02)00717-3.
17. **Chen, H.; Zhao, G.Q.; Zhang, C.S.; Liu, J.W.** 2010. Effects of Welding Chamber Step on Extrusion Process of a Complex Hollow Profile, Advanced Materials Research 148-149: 1684-1688. https://doi.org/10.4028/www.scientific.net/AMR.148-149.1684.
18. **Yu, J.; Zhao, G.; Chen, L.** 2016. Analysis of longitudinal weld seam defects and investigation of solid-state bonding criteria in porthole die extrusion process of aluminum alloy profiles, Journal of Materials Processing Technology 237: 31-47. http://dx.doi.org/10.1016/j.jmatprotec.2016.05.024.
19. **Ma, S.C.; Mun, S.D.; Choi, Y.** 2022. A study on the properties of welding-line in aluminum extrusion process, Journal of Mechanical Science and Technology 36(12): 5939-5945. https://doi.org/10.1007/s12206-022-1110-x.
20. **Wang, Y.; Wells, M.A.** 2023. The Effect of the Bridge's Angle during Porthole Die Extrusion of Aluminum AA6082, Metals 13(3): 605. https://doi.org/10.3390/met13030605.
21. **Ayer, Ö.; Karakaya, I.** 2023. Investigation of welding quality and internal elongation problem in aluminum extrusion, Journal of Manufacturing Processes 106: 254-264. https://doi.org/10.1016/j.jmapro.2023.10.001.
22. **Hwang, Y.M.; Hsu, I.P.** 2023. Die Design and Finite Element Analysis of Welding Seams during Aluminum Alloy Tube Extrusion, Metals 13(5): 911. https://doi.org/10.3390/met13050911.
23. **Liu F.; Sun L.; Zhao G.; Sun X.; Wang Y.; Jin W.; Ma Y.; Zhang B.** 2024. Microstructure and mechanical properties of longitudinal weld in 6005A aluminum alloy profile extruded by a porthole die, Journal of Materials Research and Technology 28: 2552-2571. https://doi.org/10.1016/j.jmrt.2023.12.182.

24. **Zhang, C.; Zhao, G.; Guan, Y.; Gao A.; Wang L.; Li P.** 2015. Virtual tryout and optimization of the extrusion die for an aluminum profile with complex cross-sections, International Journal of Advanced Manufacturing Technology 78: 927-937.
https://doi.org/10.1007/s00170-014-6691-9.
25. **Yi, J.; Wang, Z.; Liu, Z.; Zhang, J.; He, X.** 2018. FE analysis of extrusion defect and optimization of metal flow in porthole die for complex hollow aluminum profile, Transactions of Nonferrous Metals Society of China 28(10): 2094-2101.
https://doi.org/10.1016/S1003-6326(18)64853-8.
26. **Giarmas, E.; Tzetsis, D.** 2022. Optimization of die design for extrusion of 6xxx series aluminum alloys through finite element analysis: a critical review, International Journal of Advanced Manufacturing Technology 119: 5529-5551.
https://doi.org/10.1007/s00170-022-08694-3.
27. **Jajimoggala, S.** 2018. Selection of Optimal Hot Extrusion Process Parameters for AA6061-Fly Ash Composites: Using Simulation, International Journal of Materials Forming and Machining Processes 5(1): 52-67. https://doi.org/10.4018/IJMFMP.2018010104.
28. **Zhang, C.; Zhao, G.; Chen, H.; Guan, Y.; Li, H.** 2012. Optimization of an aluminum profile extrusion process based on Taguchi's method with S/N analysis, International Journal of Advanced Manufacturing Technology 60: 589-599.
https://doi.org/10.1007/s00170-011-3622-x.

Y. Saral, S. O. Eruslu, I. S. Dalmis

DESIGN OF THE COMPLEX ALUMINUM BRIDGE EXTRUSION DIE THROUGH FINITE ELEMENT ANALYSIS

S u m m a r y

In this study, the aluminum bridge die extrusion process for AA6061 alloy was investigated using a coupled thermomechanical finite element analysis (FEA) combined with industrial extrusion experiments. The process parameters, including die temperature, ram speed, billet diameter, and billet length, were defined according to industrial production conditions. Unlike conventional approaches that evaluate die parameters separately, this study presents an integrated optimization of a complex bridge die by simultaneously modifying baffle plates, pocket geometry, and bearing lengths.

The numerical model was used to analyze the temperature and velocity distributions at the die exit and to evaluate stress levels within the bridge die structure. The initial die design exhibited severe flow imbalance, characterized by a high velocity relative difference (VRD ≈ 25.3%) and excessive exit temperatures, which led to profile bending, dimensional deviations, and insufficient welding pressure.

Through systematic design modifications, the optimized die configuration significantly improved the flow balance, reducing the VRD to approximately 4.6% while maintaining exit temperatures within the desired range. The improved metal flow also increased the welding pressure and enhanced the dimensional stability of the extruded profile. Mechanical tests confirmed the effectiveness of the optimized design, showing increases in tensile strength and yield strength, as well as a more uniform hardness distribution across profile regions with varying thickness.

The results demonstrate that a coordinated optimization of baffle plates, pocket geometry, and bearing lengths is essential for achieving balanced metal flow and high weld quality in bridge die extrusion. The combined numerical–experimental approach provides a reliable methodology for improving the performance and structural reliability of complex aluminum extrusion dies used in industrial production.

Keywords: aluminum extrusion die, aluminum profile, finite element method, simulation.

Received March 19, 2026
Accepted June 19, 2026